Journal of New Materials for Electrochemical Systems 14, 043-049 (2011)

Improving the Sensitivity of a Mass Sensor for Azo Dye using Metal Films Modified Silver/Quartz and Gold /Quartz Electrodes

Lai-Hao Wang* and Yi-Chieh Li

Department of Medical Chemistry, Chia Nan University of Pharmacy and Science
60 Erh-Jen Road, Section 1, Jen Te, Tainan 71743, Taiwan

Received: October 30, 2010, Accepted: January 7, 2011, Available online: February 15, 2011

Abstract: *We electroreduced azo dye (D&C orange No. 4; e.g. "Drug and Cosmetic" No. 4) on silver (Ag)/quartz and gold (Au)/quartz, electrochemically deposited it on various metal films (lead (Pb), zinc (Zn), copper (Cu), tin (Sn), antimony (Sb), and cadmium (Cd) on Ag /quartz and Au/quartz substrates, and investigated it using electrochemical quartz crystal microbalance (EQCM) analysis with AT-cut quartz crystals (9-MHz). We found that the electrocatalytic property of antimony was better than that of the other metals tested. In addition, atomic force microscopy (AFM) and scanning electron microscopy (SEM) images clearly showed the structure of the adsorbed D&C orange No. 4 molecule layers on metal-modified Ag/quartz and Au/quartz electrodes.*

Keywords: Azo dye; Ag/quartz and Au /quartz electrodes; metal film- Ag/quartz and Au/quartz electrodes.

1. INTRODUCTION

Azo dyes are so named because they contain a molecular group consisting of one or more azo group (−N=N−) bridges linking substituted aromatic structures. Today, azo colorants account for more than 40% of the world's production of organic colorants. At least 3000 kinds of azo dyes have been used for various purposes in the textile, leather, food, pharmaceutical, and cosmetics industries [1-2].A significant attribute of the EQCM is its ability to provide correlations between electrochemistry induced mass changes at the electrode surface and charge consumed in the process. Such measurements aid in determination of composition of the deposit, its stoichiometry, and the efficiency of the usage of charge in its deposition [3]. Electrochemical quartz crystal microgravimetry (EQCM) is ideally suited to the study of metal deposition reactions, such as copper and silver [4-5], cobalt [6], mercury [7], lead [8], nickel [9-10] copper-selenium [11], and copper-cobalt alloy [12], nickel-cobalt oxide film [13] and ternary CuAgSe film [14]. There is, however, only one report on this EQCM [15], on the electrochemical reduction of Mordant Red 19 done on mercury (Hg) films on gold and on the polypyrrole layer. D&C orange No. 4 is one of azo dyes. Both azobenzene and hydrobenzene are known to be adsorbed on mercury electrode. Gold has been employed in most EQCM studied, but it has certain limitations, such as a lower overpotential for hydrogen evolution compared to mercury or glassy carbon, a narrower potential window, and a poorer adsorptivity for organic molecules. Therefore, deposition of metals on Au/quartz and Ag/quartz were investigated by EQCM respectively which metals modified electrodes to study the adsorption/desorption of D&C orange No. 4.

2. EXPERIMENTAL

2.1. Materials and apparatus

Metal materials were: lead (II) nitrate (Acros), zinc acetate (J.T.Baker), cadmium acetate(Shimakyus pure chemicals), copper(II) nitrate (Aldrich), tin (II) acetate (Alta Aesar) , and antimony (III) acetate (Sterm Chemicals).

The sample of 4-[(2-hydroxy-1-naphthyl)azo]benzenesulfonic acid, monosodium salt (D&C Orange No. 4; C.I. 15510) was from Sensient Cosmetic Technologies/LCW (Milwaukee, WI, USA). Other chemical reagents used were of analytical grade.

The EQCM system used for the experiments consisted of a potentiostat/galvanostat (263A; EG&G Princeton Applied Research, Princeton, NJ, USA) coupled to a quartz crystal analyzer (QCA 922; Seiko EG&G Co., Ltd., Chiba, Japan). The QCM cell was home-made and connected to well-type quartz crystal holder (QA-

*To whom correspondence should be addressed: Email: 201466.wang@msa.hinet.net

Abbreviation: Drug and Cosmetic orange No. 4 (D&C orange No. 4).

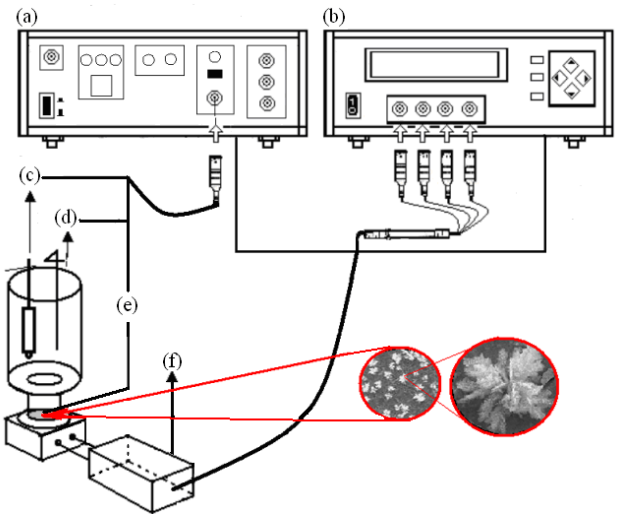

Scheme 1. Schematic representation of the experimental set up (QCM cell was home-made). (a) potentiostat / galvanostat; (b) quartz crystal analyzer; (c) Ag/AgCl reference electrode; (d) platinum counter electrode; (e) Sb modified Ag/ quartz working electrode; (f) quartz crystal holder.

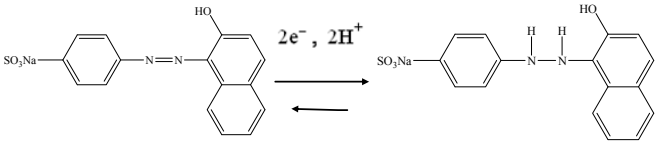

Scheme 2.

CL4; Seiko).The crystal was mounted in the holder and connected with an adapter cable (QCA 922-10; Seiko). A schematic of the experimental set-up is shown in Scheme1. When the quartz crystal was immersed into the solution, only one side of it was exposed to the electrolyte solution; that side was used as the sensing surface that enabled measurements of small changes in mass and viscosity of the liquid. The 9-MHz quartz crystal with a 300-nm layer of gold or silver sputtered onto a 100-nm layer of titanium used for the working electrode substrate (geometric area: 0.196 cm^2) was also purchased from Seiko. A platinum wire counter and an Ag/AgCl reference electrode (RE-1; Bioanalytical Systems, Inc. (BAS), West Lafayette, IN, USA) completed the electrochemical set-up (Scheme 1).

2.2. Working electrodes

Two types of Au / quartz and Ag/ quartz electrodes were used for the EQCM measurements: (i) metals (lead, zinc, copper, tin, antimony, and cadmium) were deposited potentiostatically onto the Ag and Au electrodes of the quartz; and (ii) bright commercial Ag /quartz and gold /quartz electrodes, which was exposed to 0.1 M acetate buffer, and the resonance frequency of the quartz was monitored. QCM crystals were covered with a thin layer of metals and were the subsequent voltammetric studies. D&C Orange No. 4 accumulated on M/Au quartz and M/Ag quartz between 0.2 V and –1.0 V, and sweep rate at 25 mV/s.

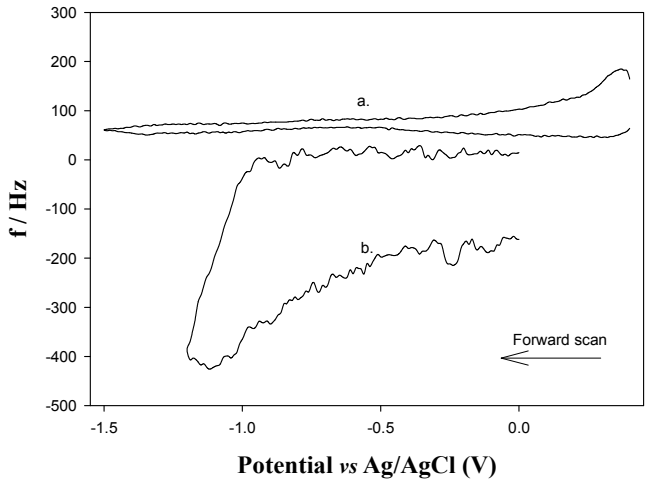

Figure 1A. Frequency of (a) Ag/quartz and (b) Au/quartz electrodes in 0.1 M acetate buffer solution, sweep rate at 25 mV/s.

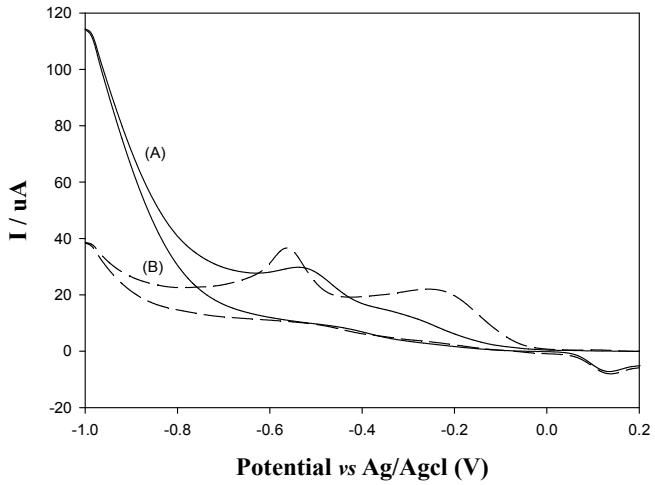

Figure 1B. Cyclic voltammograms of D&C Orange No. 4 (4.34×10^{-4} M) at a different (A *solid line*) Au / quartz, and (B *circle line*) Ag /quartz, electrodes in 0.1 M acetate buffer solution, sweep rate at 25 mV/s.

3. RESULTS AND DISCUSSION

3.1. Behavior of D&C orange No. 4 on Ag/quartz and Au/quartz

Electrochemical reduction of D&C Orange No. 4 was proposed to occur in $2e^-$ and 2 H^+ process to give hydrazo products and shown in Scheme 2. Frequency changes at Au/quartz and Ag/quartz electrodes in 0.1 M acetate buffer solution were shown in Fig. 1A. Frequency decreases at Au/quartz was higher than that at Ag/quartz. Fig. 1B depicts the cyclic voltammogram (CV) of D&C Orange No. 4 (4.34×10^{-4} M) on Au (Seiko), and Ag (Seiko) quartz crystals electrodes with potentials ranging between 0.2 V and -1.0 V, respectively. Fig. 1B shows the reduction of D&C Orange No. 4 and its stripping -0.54 V and -0.56 V on Au/quartz and Ag/quartz,

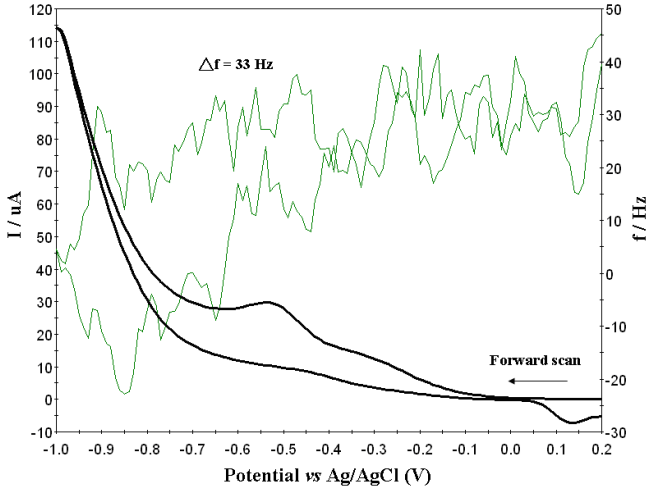

Figure 2A. Potentiodynamic simultaneous recording of the current and frequency of D&C Orange No. 4 (4.34×10^{-4} M) on Au /quartz electrode in 0.1 M acetate buffer solution (sweep rate: 25 mV/s).

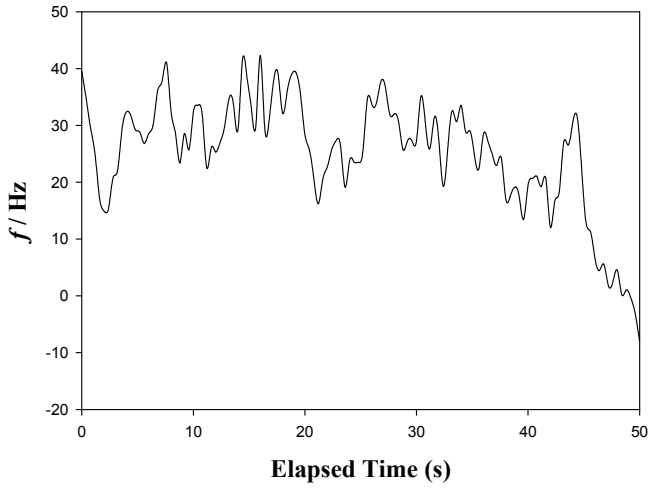

Figure 2B. Frequency shifts, $\Delta f \sim t$ (s) of D&C Orange No. 4 (4.34×10^{-4} M) on Au /quartz electrode in 0.1 M acetate buffer solution (sweep rate: 25 mV/s).

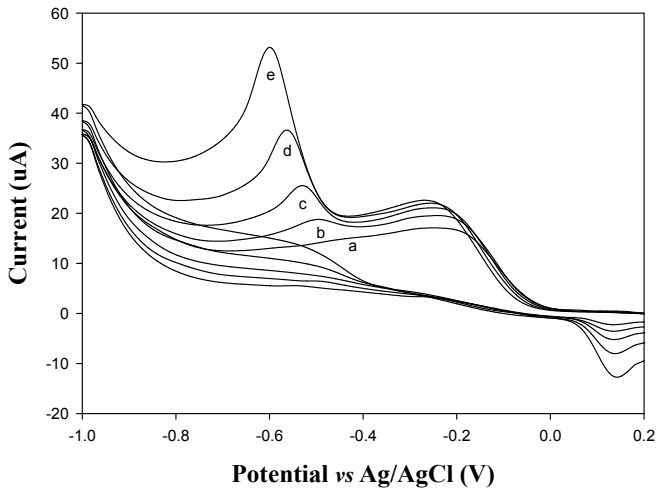

Figure 3. Cyclic voltammograms of different concentrations at a Ag/ quartz electrode and related current-concentration curve: (a) 0.567×10^{-5} M; (b) 1.127×10^{-4} M;(c) 2.22×10^{-4} M (d) 4.34×10^{-4} M ; (e) 8.25×10^{-4} M in 0.1 M acetate buffer solution, sweep rate at 25 mV/s.

respectively. The potential at -0.21 V showed the background response in acid electrolyte due to coadsorption of acetate oxyanion. However, D&C Orange No. 4 reduction peak was not affected by the value of background potential [16]. The reduction process was found irreversible in nature on the basis of the shift of the cathodic peak potential toward more negative potential with the increasing sweep rate and absence of any peak in reverse scan. The adsorption of the D&C Orange No. 4, on Au/quartz is characterized by a broad voltammetric wave, which becomes sharper wave on Ag/quartz. The voltammetric wave occurring at more positive potential is due to disorder-to-order phase transition at higher surface coverage. Evidence supporting this interpretation is obtained from an in-situ EQCM measurement of the interfacial frequency associated with voltammetric wave.

At -0.54 V the reduction peak and the corresponding frequency decrease were observed (Fig. 2). The simultaneous $\Delta f \sim E$ plot was shown in Fig. 2A. Fig. 2B was the plot of $\Delta f \sim t$ (s), Δf_{48} is lower than that of Δf_0, it means frequency decreased during the CV process, which means D&C Orange No. 4 was adsorbed onto the electrode. From potential 0.2 to -1.0 V, frequency decreases, i.e., when D&C Orange No. 4 is reduced. Table 1 showed the cathodic currents, potentials and frequencies decrease of the D&C Orange No. 4 at various electrodes. While the peak potential at the Au/quartz electrode is slight more positive and frequency decrease is about 2.4 times larger than that at the Ag/quartz. However, the peak current at Ag/quartz is about 1.5 times higher than that at the Au/quartz electrode. After background correction, the decrease in frequency (Δf) increase with concentration (0.22 mM and 0.44 mM), and (Δf) was calculated to be 14 Hz and 33 Hz for Ag/quartz and Au/quartz electrodes, respectively.

The CV obtained using the standard addition method (the regression equations used were [y = 0.1222 x + 11.16; correlation coefficient (r) = 0.9998] and [y = 0.1387 x + 16.37; r = 0.9990] for

Table 1. Cyclic voltammetric results and frequency of azo dye D&C orange No. 4 on Au/quartz and Ag/quartz electrodes

Electrodes	- E_p(V)		i_p (μA)		Decrease f (Δ Hz)	
	0.22 mM	0.44 mM	0.22 mM	0. 44 mM	0.22 mM	0.44 mM
Au/quartz	0.51 ± 0.01	0.53 ± 0.01	15 ± 6.0	25 ± 7.0	14 ± 4.5	33 ± 15
Ag/quartz	0.56 ± 0.07	0.59 ± 0.06	25 ± 0.8	37 ± 2.0	2.3 ± 0.8	14 ± 1.8

Supporting electrolyte: 0.1 M acetate buffer; scan rate: 25 mV/s.

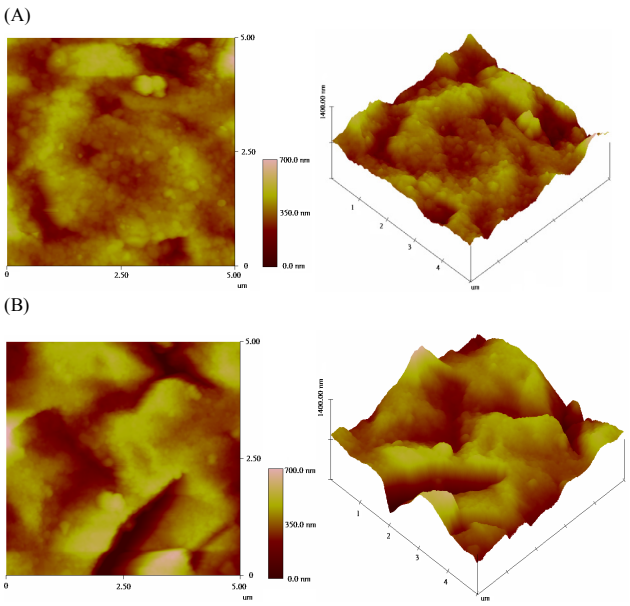

Figure 4. AFM 2D and 3D images of (A) silver/quartz; (B) azo dye/silver quartz.

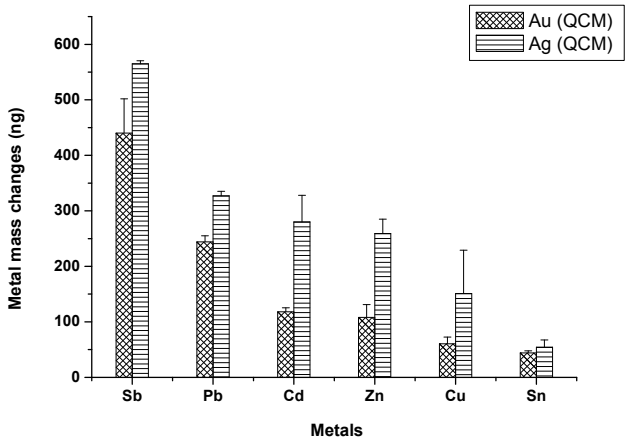

Figure 5. Mass changes for deposition of metals on Au /quartz and Ag /quartz electrodes from an 0.1 M acetate buffer solution.

Au/quartz and Ag /quartz electrodes, respectively) showed a well-defined reduction peak. The calibration graphs were linear for Orange No. 4 over the range of concentrations used. Fig. 3 for Ag /quartz electrode showed a well-defined reduction peak from - 0.49 V shift to - 0.60 V increase with concentrations used (0.567 - 8.25 ´ 10^{-4} M). The adsorption of D&C Orange No. 4 to Ag/quartz was also examined using atomic force microscopy (AFM) (NanoMan NS4+D3100; Digital Instrument Company, Taipei, Taiwan) (Fig. 4). Rather than a film surface of uniform thickness (Fig. 4A), the azo dye absorption formed an island (Fig. 4B).

3.2. Behavior of D&C orange No. 4 on metals/ Ag/quartz and metals/Au/quartz

Electrochemical cyclic voltammetry and EQCM for solution-

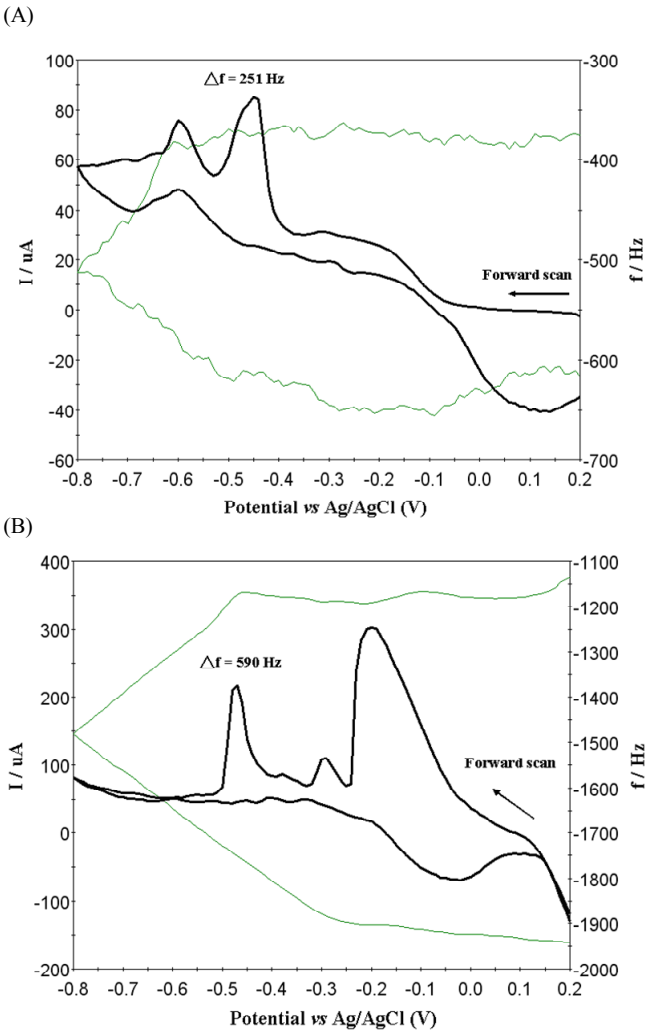

Figure 6. Potentiodynamic simultaneous recording of current and frequency of deposition (A) Sb/Au/quartz;(B)Sb/Ag /quartz electrodes in 0.1 M acetate buffer solution (sweep rate: 25 mV/s).

based deposit characterization is a standard method in solid liquid interfacial surface science [17-18]. For comparision, thin films of metal (Zn, Pb, Sb, Cu, Cd, and Sn) were deposited on the Ag/quartz and Au/quartz electrodes. Comparative in EQCM studies on the electrodeposition of metal film and voltammetric data could be to express the equation: $i(t) = -\frac{KnF}{AM} \bullet \frac{d\Delta f}{dt}$ Where M is the molar mass of deposited metal, n is the number of electrons transferred to the metal ion, F is Faraday's constant, A is the electrochemically active area, f is the frequency, t is time. The sense of k is evident from the equation: $\Delta m = -k\,\Delta f$.

Fig. 5 compares the mass changes during metal deposition on Ag/quartz and Au/quartz electrodes. The change in weight, Δm, was calculated from the change in frequency, Δ*f*, using the Sauerbrey equation [19]. The amounts of deposited metal were calculated to be 440- 44 ng and 565- 54 ng from the frequency change on Au/quartz and Ag/quartz electrodes, respectively. The mass changes of both Ag and Au electrodes, the order is Sb > Pb > Cd > Zn > Cu > Sn. The mass change of metal (Zn, Pb, Sb, Cu, Cd, and

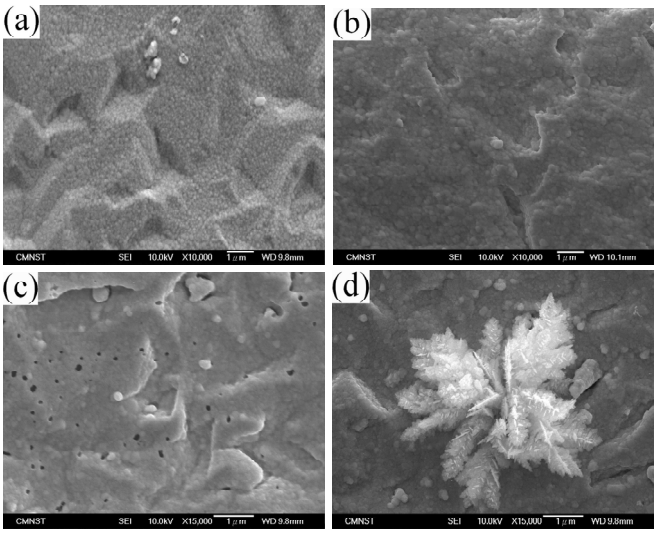

Figure 7A. SEM (at 10 kV) of metal particles distribution in the Ag surfaces: (a) Cd /Ag (b) Pb/Ag(c) Zn/Ag (d) Sb/Ag alloy EQCM electrodes

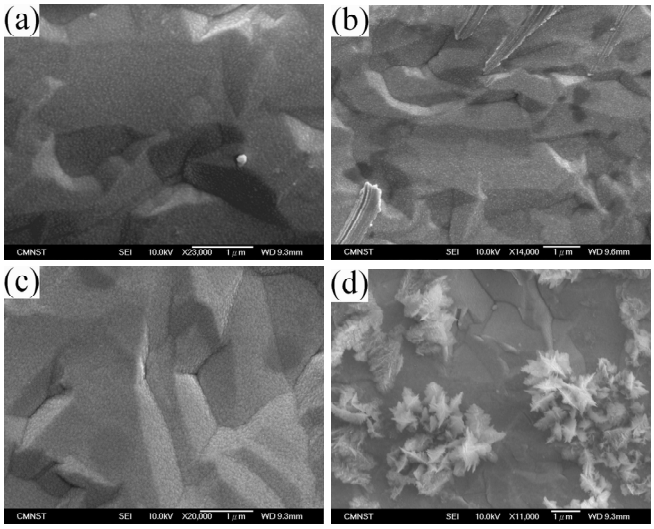

Figure 7B. SEM (at 10 kV) of metal particles distribution in the Au surfaces: (a) Cd /Au (b) Pb/Au(c) Zn/Au (d) Sb/Au alloy EQCM electrodes.

Sn) on Ag/quartz is higher than Au/quartz. Fig. 6A compared with Fig. 6B, shows representatively Sb-Au/quartz and Sb-Ag/quartz frequency and cyclic voltammograms. Frequency-shift data and CVs recorded at Au- and Ag-coated quartz crystal electrodes as a function of scanning potential in 0.1 M acetate buffer solution shows that the frequency responses changed significantly for Pb, Sb, Cd, and Zn depositions. Scanning electron microscope (SEM) micrographs may give a direct image of the surface of thin-film electrodes. Four field emission scanning electron microscope (FE-SEM) (JSM-7000; JEOL, Akishima City, Tokyo, Japan) photos of modified electrode substances are shown in Fig. 7A and B. The size and shape Pb, Cd, and Zn of deposited particles are similar uniform distribution covering the surface on Ag /quartz and Au/quartz. Fig. 7d show the small rod shape particles with large flower-leaf shape clusters, which might be related to the Sb metal. The reduction of the D&C Orange No. 4 on the various metal-Au /quartz and metal-Ag /quartz electrodes, which smaller peak current and more positive potential than that of bare Au /quartz and Ag /quartz electrodes, and shown in Table 2 and 3. As shown in Table 2, the peak current on the metal- Au /quartz is approximately 45μA which is about 85% of that on Au /quartz electrode. This implies that the effective area covered by metals. The electrocatalysts of Au / quartz crystal based Sb-Au, Pb-Au, Cd-Au and Zn-Au surface alloy were prepared by electrodeposition; and the reduction potential of D&C Orange No. 4 is lower than Au. From Table 2 and 3 can be seen, the lowest potential of D&C Orange No. 4 were Zn-Au/quartz (- 0.54 V) and Sb-Ag/quartz (-0.56 V), respectively. Currents of D&C Orange No. 4 on M/Au quartz were lower than that Au quartz (Table 2) due to electrodeposition of metal-Au alloys. The same as the results of M/Ag quartz and Ag quartz was shown in Table 3. Comparion with modified and bare electrode, a representative cyclic voltammograms of D&C Orange No. 4 were shown in Fig. 8A and B. The surface morphology of Sb-Ag/quartz nanoparticle hybrid film was investigated using atomic force microscopy (AFM) (Fig.9).To confirm the electroanalytical utility of Sb-Ag/quartz nano-composite electrodes, we performed electrochemical experiments in which the antimony molecules on the silver electrode had diameters between 250 nm and 500 nm.

4. CONCLUSIONS

We showed the EQCM responses from cyclic voltammograms for six electrodeposition systems (Pb, Zn, Cu, Sn, Sb, and Cd,) on Ag and Au quartz crystal electrodes. These electrodes were used to absorb the processing of azo dye D&C orange No. 4, as well as sensitive and dynamic piezoelectric sensors.

Table 2. Cyclic voltammetric results of azo dye D&C orange No. 4 on various metal- Au/quartz electrodes (concentration:8.25×10^{-4}M)

Electrodes	- E_p(V)	i_p (μA)
Au/quartz	0.61 ± 0.01	53 ± 7.6
Sb-Au/quartz	0.58 ± 0.01	44 ± 1.7
Pb- Au/quartz	0.57 ± 0.03	47 ± 3.6
Cd- Au/quartz	0.58 ± 0.04	43 ± 3.0
Zn- Au/quartz	0.54 ± 0.01	45 ± 3.3

Supporting electrolyte: 0.1 M acetate buffer; scan rate: 25 mV/s.

Table 3. Cyclic voltammetric results of azo dye D&C orange No. 4 on various metal- Ag/quartz electrodes (concentration: 8.25×10^{-4}M)

Electrodes	- E_p(V)	i_p (μA)
Ag/quartz	0.67 ± 0.05	57 ± 2.8
Sb- Ag/quartz	0.56 ± 0.06	48 ± 9.0
Pb- Ag/quartz	0.65 ± 0.03	48 ± 6.3
Cd- Ag/quartz	0.60 ± 0.03	45 ± 1.9
Zn- Ag/quartz	0.61 ± 0.01	47 ± 4.3

Supporting electrolyte: 0.1 M acetate buffer; scan rate: 25 mV/s.

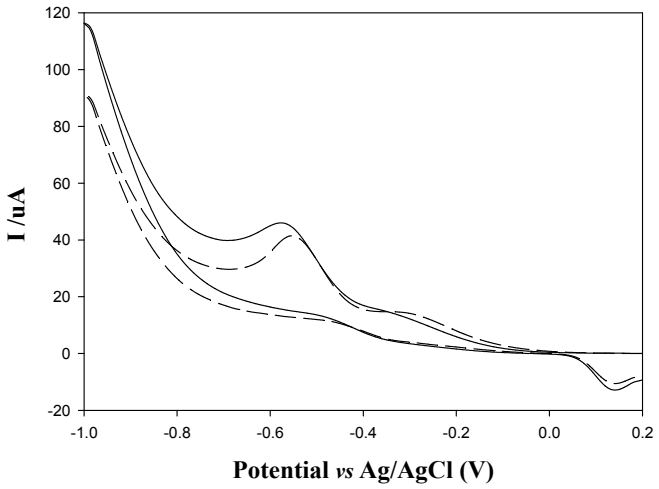

Figure 8A. Cyclic voltammograms of D &C Orange No. 4 (8.25 ´ 10^{-4} M) at a different (solid line) Au / quartz, and (circle line) Zn-Au /quartz, electrodes in 0.1 M acetate buffer solution, sweep rate at 25 mV/s.

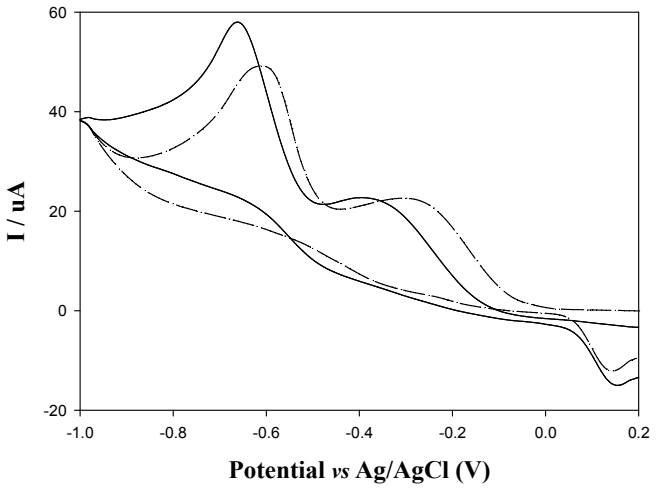

Figure 8B. Cyclic voltammograms of D&C Orange No.4 (8.25×10^{-4} M) at a different (solid line) Ag / quartz, and (circle line) Sb- Ag /quartz, electrodes in 0.1M acetate buffer solution, sweep rate at 25 mV/s.

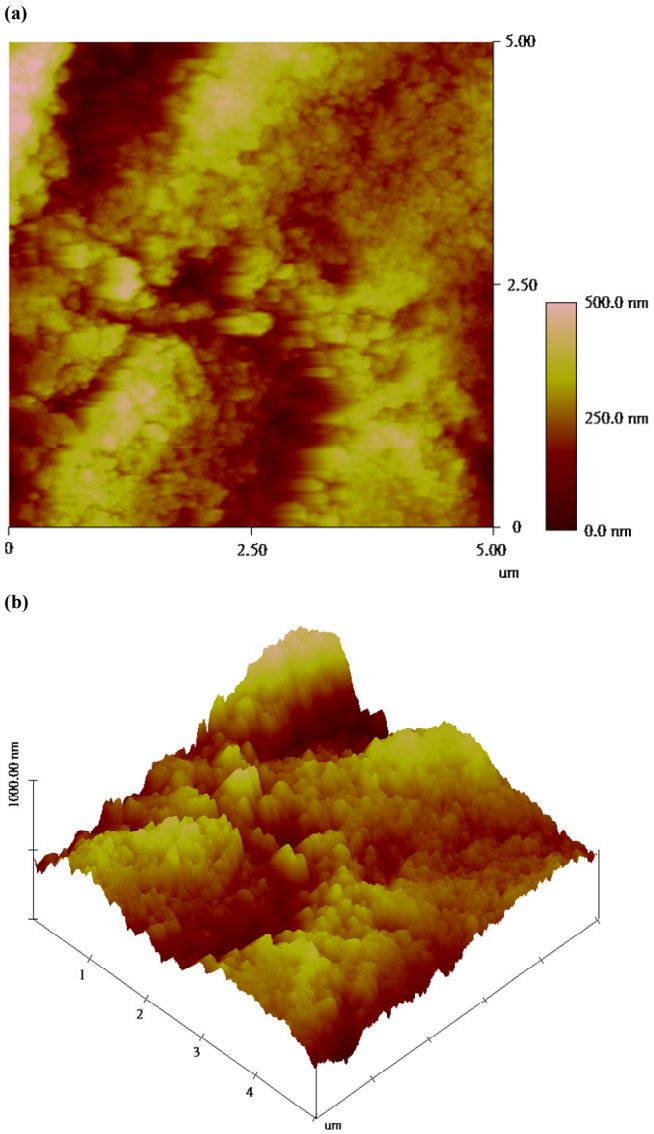

Figure 9. AFM (a)2D and (b)3D images of Sb(1 mM)/Ag/quartz.

5. ACKNOWLEDGMENTS

This work was financially supported by grant National Science Council of the Republic of China (NSC 95-2113-M-041-002).

REFERENCES

[1] Venkataraman K., The analytical chemistry of synthetic dyes:Analysis of food, drug and cosmetic colors. John Wiley & Sons, New York, 1976.

[2] Lake L.R., Indirect food additives: adjuvants, production aids, and sanitizers. Fed Regist 64, 1999.

[3] Ward M.D., Buttry D.A., Sci., 249, 1000 (1999).

[4] Jeffrey C.A., Storr W.M., Harrington D.A., J. Electroanal. Chem., 569, 61 (2004).

[5] Borges G.L., Kanazawa K.K., Gordon J.G., Ashley K., Richer J., J. Electroanal. Chem., 364, 281 (1994).

[6] Matsushima J.T., Trivinho-Strixino F., Pereira E.C., Electrochim. Acta, 51, 1960 (2006).

[7] Evans C.D., Nicic I., Chambers J.Q., Electrochim. Acta, 40, 2611 (1995).

[8] Herzog G., Srrigan D.W.M., Electroanal. Chem., 17, 1816 (2005).

[9] Lachenwitzer A., Magnssen O.M., J. Phys. Chem., B104, 7424 (2000).

[10]Song K.D., Kim K.B., Han S.H., Lee H.K., Electrochem. Commun., 5, 460 (2003).

[11]Marlot A., Vedel J., J. Electrochem. Soc., 146, 177 (1999).
[12]Kelly J.J., Kern P., Landolt D., J. Electrochem. Soc., 147, 3725 (2000).
[13]I. Serebrennikova I., Birss V.I., J. Electroanal. Chem., 493, 108 (2000).
[14]Neshkova M.T., Nikolova V.D., Bond A.M., Petrov V., Electrochim. Acta., 50, 5606 (2005).
[15]Cho K.C., Yoon S.K., Jung M.C., Kim H., Colloid and Surf., A134, 59 (1998).
[16]Sterenson K.J., Gao X.P., Hatchett D.W., White H.S., J. Electroanal. Chem., 47, 43 (1998).
[17]Oden P.I., Thundat T., Warmack R.T., Scanning microscopy, 12, 449 (1998).
[18]Saloniemi H., Kemell M., Ritala M., Leskelia M., J. Mater. Chem., 10, 519 (2000).
[19]Sauerbrey G., Phys., 155, 206 (1959).